Touching Triangle Representation for 3-Connected Planar Graphs

Stephen G. Kobourov[§], Debajyoti Mondal[‡], and Rahnuma Islam Nishat[†]

[§]Department of Computer Science, University of Arizona
[‡]Department of Computer Science, University of Manitoba
[†]Department of Computer Science, University of Victoria
kobourov@cs.arizona.edu, jyoti@cs.umanitoba.ca, rnishat@uvic.ca

Abstract. A touching triangle graph representation (TTG) of a planar graph is a planar drawing Γ of the graph, where each vertex is represented as a triangle and each edge e is represented as a side contact of the triangles that correspond to the endvertices of e. We call Γ a proper TTG if Γ determines a tiling of a triangle, where each tile corresponds to a distinct vertex of the input graph. In this paper we prove that every 3-connected cubic planar graph admits a proper TTG. We also construct proper TTG for parabolic grid graphs and the graphs determined by rectangular grid drawings (e.g., square grid graphs). Finally, we describe a fixed-parameter tractable decision algorithm for testing whether a 3-connected planar graph admits a proper TTG.

1 Introduction

Planar graphs are of interest in theory and in practice as they correspond to naturally occurring structures, such as skeletons of convex polytopes and duals of maps, and contain subclasses of interest, such as trees and grids. While traditionally graphs are represented by node-link diagrams, alternative representations also have a long history. There is a large body of work about representing planar graphs as contact graphs, i.e., graphs whose vertices are represented by geometric objects with edges corresponding to two objects touching in some specified fashion. Early results, such as Koebe's 1936 theorem [11] that all planar graphs can be represented by touching disks, deal with *point contacts*. Similarly, de Fraysseix *et al.* [6] construct representation of planar graphs with vertices as triangles, where the edges correspond to point contacts between triangles.

In this paper, we consider *side contact* representations of graphs, where vertices are represented by simple polygons, with an edge occurring whenever two polygons have non-trivially overlapping sides. The algorithms of He [10] and Liao *et al.* [12] produce side contact representations for planar graphs, with nodes represented by the union of at most two isothetic rectangles, or non-convex octagons. Bonichon *et al.* [3] and Duncan *et al.* [8] independently show that this can be done with convex hexagons, and Duncan *et al.* [8] prove that six sides are necessary for general planar graphs.

Certain subclasses of planar graphs admit even simpler side contact representations. Buchsbaum *et al.* [4] give an overview on the state of the art concerning rectangle contact graphs, which are often referred to as rectangular layouts. Graphs allowing rectangular layouts have been fully characterized [4, 14, 15] with linear-time constructive algorithms.

The simplest possible side-contact representation of a graph, in terms of the complexity of polygons used, is the triangle contact representation. Gansner *et al.* [9] show certain necessary and sufficient conditions for such representations, however a complete characterization turns out to be surprisingly difficult and is not yet known. It is known that every outerplanar graph admits a touching triangle representation (TTG) that may not be proper, and every graph that is a weak dual of some maximal planar graph admits a proper TTG [9].

In this paper we examine only the proper TTG representations, i.e., the TTG must determine a tiling of some triangle and every tile must correspond to a distinct vertex of the input graph; see Figs. 1(a–b). Recently, Alam *et al.* [1] give a characterization for the outerplanar graphs that admit proper TTG. Phillips [13] enumerates all possible tiling of a triangle into five subtriangles, which helps us to list all non-isomorphic connected planar graphs with less than six vertices that do not admit proper TTG; see Fig. 1(g).

Our Contributions: We prove that every 3-connected cubic planar graph admits a proper TTG, with an algorithm that constructs such a representation. We then show that parabolic grid graphs and the graphs determined by rectangular grid drawings (e.g., square grid graphs) have proper TTG. Finally, we describe a fixed-parameter tractable decision algorithm for testing whether a 3-connected planar graph with n vertices admits a proper TTG. We use the maximum degree Δ, the number of outer vertices and the number of inner vertices with degree greater than three as fixed parameters. Specifically, if $\Delta = 4$, then this can be done in $O^*(4^{k_1}6^{k_2})$ time[1], where k_1 is the number of degree-4 inner vertices and k_2 is the number of vertices on the outerface, which results in a polynomial-time algorithm when $k_1 + k_2 = O(\log n)$.

2 Preliminaries

A *weak dual* of a planar graph G is a subgraph induced by the vertices of the dual graph of G that correspond to the inner faces of G. The weak dual D of every maximal planar graph M is a subcubic planar graph, where only three vertices of D have degree two. Therefore, by definition any straight-line drawing of M is a proper TTG of D. Constructing a proper TTG for a 3-connected cubic planar graph G may initially seem easy since it differs from the dual of a maximal planar graph by only one vertex. But a careful look at Figs. 1(c–f) reveals that it is not obvious how to construct a proper TTG of a 3-connected cubic planar graph from its corresponding maximal planar graph.

A *straight-line drawing* Γ of a planar graph G is a planar drawing of G, where each vertex is drawn as a point and each edge is drawn as a straight line

[1] O^* ignores the polynomial terms.

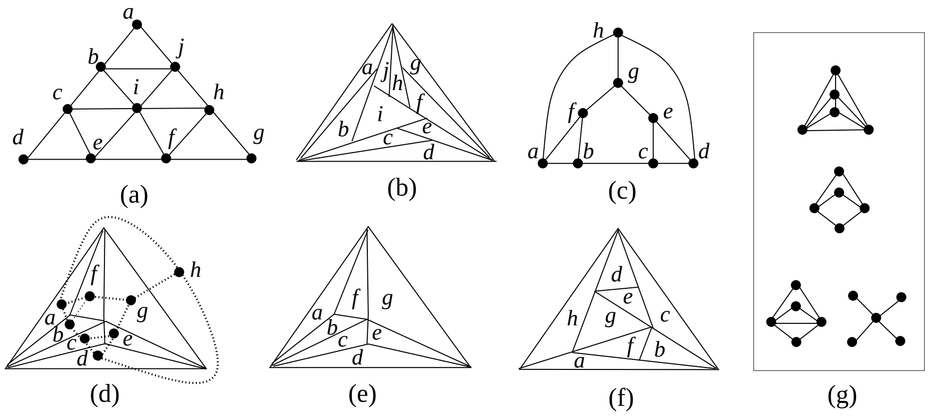

Fig. 1. (a) A planar graph G. (b) A proper TTG of G. (c) A 3-connected cubic planar graph G'. (d) The dual graph M of G', where G is shown in dotted lines. (e) A straight-line drawing of M is a proper TTG of its own weak dual. (f) A proper TTG of G'. (g) All planar graphs with less than six vertices that do not admit proper TTG.

segment. A path $v_1, v_2, \ldots, v_k$ is *stretched* in Γ if all the vertices on the path are collinear in Γ. Two paths are *non-crossing* if they do not have an internal vertex in common. A *path covering* of G is an edge covering of G by non-crossing edge-disjoint paths.

Theorem 1 (de Fraysseix and de Mendez [5]). *A path covering $\mathcal{P}$ of a plane graph $\mathcal{G}$ is stretchable if and only if each subset $\mathcal{S}$ of $\mathcal{P}$ with at least two paths has at least three free vertices, where a free vertex in the graph H induced by $\mathcal{S}$ is a vertex on the outerface of H that is not internal to any path of $\mathcal{S}$.*

By a *k-cycle* in G we denote a cycle of k vertices in G. By $\text{len}(f)$ we denote the length (i.e., the number of vertices on the boundary) of a face f of G.

Throughout the paper we only examine the proper touching triangle representations. Therefore, unless explicitly stated otherwise, by the term "TTG" we denote a proper touching triangle representation. We also assume that the combinatorial embedding of the input graph is fixed, i.e., the input is a *plane graph.*

3 Proper TTG of 3-Connected Cubic Planar Graphs

In this section we describe an algorithm for constructing a proper TTG of a 3-connected cubic planar graph G based on the combinatorial structure of such graphs. In particular, every 3-connected cubic planar graph can be constructed starting with a K_4 and then applying one of the three "growth" operations [2]; see Figs. 2(a–c). We use this inductive construction of 3-connected cubic planar graphs to construct its TTG. While constructing G, we maintain a plane graph G' that corresponds to the TTG of G. We also define a path covering $P(G')$ of

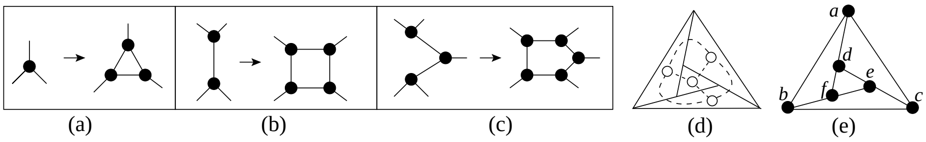

Fig. 2. (a–c) Growth operations 1–3; (d) $G = K_4$ and its proper TTG; (e) G'.

G' such that any planar embedding of G' with every path in $P(G')$ stretched, is a TTG of G. We now describe our algorithm in details.

We start with $G = K_4$, and the graph G' that corresponds to the TTG of G; see Figs. 2(d–e). Throughout the algorithm G' will have exactly three inner faces incident to its three outer edges, each of which is a 4-cycle. We call these faces the *quads* of G'. For every quad we will define a *stick*, which is a path of three vertices on the corresponding quad. No two sticks in G' will have an edge in common. All the inner faces of G' other than the quads will be 3-cycles, which we call the *ordinary faces*.

In Fig. 2(e), the 4-cycles $[a, b, f, d]$, $[b, c, e, f]$ and $[c, a, d, e]$ are the quads of G', where $\langle a, d, f\rangle$, $\langle b, f, e\rangle$ and $\langle c, e, d\rangle$ are their sticks, respectively. The *path covering* $P(G')$ consists of the sticks and all the edges of G' that are not covered by the sticks. In Fig. 2(e), the path covering $P(G') = \{\langle a, d, f\rangle, \langle b, f, e\rangle, \langle c, e, d\rangle, \langle a, b\rangle, \langle b, c\rangle, \langle c, a\rangle\}$.

Assume inductively that we have a 3-connected cubic planar graph $\mathcal{G}$, its corresponding graph $\mathcal{G}'$ and path covering $P(\mathcal{G}')$, where one of the three growth operations of Figs. 2(a–c) on $\mathcal{G}$ produces the input graph G. In Lemmas 1–3 we show how to construct the graph G' and its path covering $P(G')$ by a constant number of insertion/deletion on $\mathcal{G}'$ and $P(\mathcal{G}')$, respectively.

Lemma 1. *Assume that G is produced from $\mathcal{G}$ by an application of Operation 1. Then the graph G' and its path covering $P(G')$ can be constructed by a constant number of insertion/deletion on $\mathcal{G}'$ and $P(\mathcal{G}')$, respectively.*

Proof. First consider the case when vertex v of $\mathcal{G}$, on which we apply Operation 1, corresponds to an ordinary face T of $\mathcal{G}'$. We then add a vertex x inside T and connect the vertex with the three vertices on the boundary of T. Let the resulting graph be G'. It is easy to verify that the vertices on the cycle that replaces v correspond to the three new ordinary faces in G'; see Figs. 3(a–b). The path cover $P(G')$ consists of all the paths of $P(\mathcal{G}')$ along with the three paths that correspond to the three new edges incident to x.

Next consider the case when vertex v of $\mathcal{G}$, on which we apply Operation 1, corresponds to a quad $T = [a, b, c, d]$ of $\mathcal{G}'$. Without loss of generality assume that the stick of T is $\langle a, d, c\rangle$ and the outer edge of T is (b, c). We then add a vertex x inside T and add the edges $(a, x), (b, x)$ and (d, x); see Figs. 3(c–d). Let the resulting graph be G'. The 4-cycle $[b, x, d, c]$ is a quad in G' and $\langle b, x, d\rangle$ is its stick. Since $\mathcal{G}'$ contains exactly three quads, G' also contains exactly three quads (i.e., $[b, x, d, c]$ replaces $[a, b, c, d]$ and all other quads remain the same). The path cover $P(G')$ consists of all the paths of $P(\mathcal{G}') \setminus \langle a, d, c\rangle$ along with the paths $\langle a, d\rangle, \langle d, c\rangle, \langle a, x\rangle, \langle b, x, d\rangle$. □

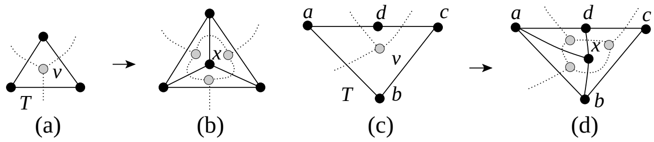

Fig. 3. (a–d) Illustration for Operation 1. $\mathcal{G}$ and G are shown in dotted lines as weak duals of $\mathcal{G}'$ and G', respectively.

Since the path covering $P(G')$ consists of the sticks and all the edges of G' that are not covered by the sticks, in Lemmas 2 and 3, we will only define the sticks in G', instead of defining $P(G')$ explicitly.

Lemma 2. *Assume that G is produced from $\mathcal{G}$ by an application of Operation 2. Then the graph G' and its path covering $P(G')$ can be constructed by a constant number of insertion/deletion on $\mathcal{G}'$ and $P(\mathcal{G}')$, respectively.*

Proof. Assume that the vertices v and u of $\mathcal{G}$ on which we apply Operation 2 correspond to two faces T_1 and T_2 of $\mathcal{G}'$. Then T_1 and T_2 must share an edge, which we denote by e'. We distinguish three cases, depending on the types of these faces.

Case 1 (T_1 and T_2 are ordinary faces): Here we subdivide e' with a vertex x and connect x with the vertices on T_1 and T_2 that are not already adjacent to x. The resulting graph is G'; see Figs. 4(a–b). The new faces are ordinary, and hence the quads and sticks of G' coincide with the quads and sticks of $\mathcal{G}'$.

Case 2 (Exactly one of T_1 and T_2 is a quad): Without loss of generality assume that the outer boundary of the union of T_1 and T_2 is a, b, c, d, e, T_1 is the quad and $\langle a, c, d\rangle$ is its stick; see Fig. 4(c). We now subdivide e' with a vertex x. If (d, e) is the outer edge, then we add the edges $(x, b), (x, e)$. Otherwise (a, e) is the outer edge and we add the edges $(x, b), (x, d)$. The resulting graph is G'; see Figs. 4(c)–(f). The quad $[a, c, d, e]$ of $\mathcal{G}'$ does not determine quad for G'. The new quad of G' is $[x, c, d, e]$ (resp., $[a, x, d, e]$), where $\langle x, c, d\rangle$ (resp., $\langle a, x, d\rangle$) is its stick, as shown in Fig. 4(d) (resp., Fig. 4(f)). The four new faces in G' correspond to the four vertices of the cycle that replace u and v of $\mathcal{G}$.

Case 3 (Both T_1 and T_2 are quads): Without loss of generality assume that the outer boundary of the union of T_1 and T_2 is a, b, c, d, e, f, and $\langle a, d, e\rangle$, $\langle b, c, d\rangle$ are the sticks of T_1, T_2, respectively. By induction, every quad in $\mathcal{G}'$ contains an outer edge. Since b and e are distinct vertices, both (a, b) and (e, f) cannot be the outer edges of $\mathcal{G}'$. Consequently, (a, b) and (a, f) are the outer edges of T_1 and T_2, respectively; see Fig. 4(g).

We now subdivide e' with a vertex x and add the edges $(x, c), (x, e)$; see Fig. 4(h). The quads $[a, b, c, d]$ and $[a, d, e, f]$ of $\mathcal{G}'$ are not the quads for G'. The quads of G' are $[a, b, c, x]$ and $[a, x, e, f]$, where $\langle b, c, x\rangle$ and $\langle a, x, e\rangle$ are their corresponding sticks. □

The following lemma examines the construction of G' and $P(G')$ for Operation 3. A detailed proof of this lemma is included in the Appendix.

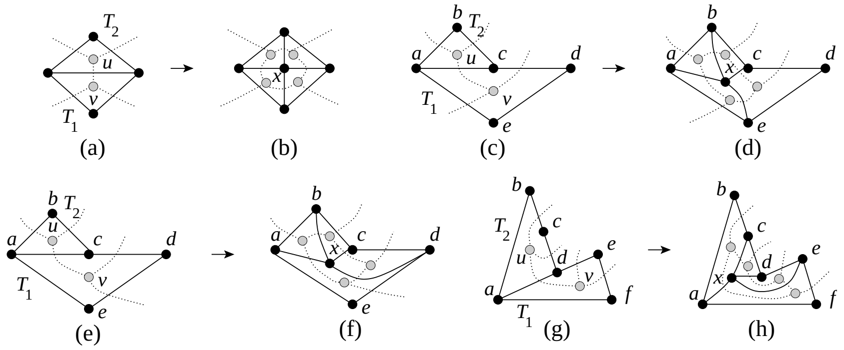

Fig. 4. (a–h) Illustration for Operation 2. $\mathcal{G}$ and G are shown in dotted lines as weak duals of $\mathcal{G}'$ and G', respectively.

Lemma 3. *Assume that G is produced from $\mathcal{G}$ by an application of Operation 3. Then the graph G' and its path covering $P(G')$ can be constructed by a constant number of insertion/deletion on $\mathcal{G}'$ and $P(\mathcal{G}')$, respectively.*

Theorem 2. *Every 3-connected cubic planar graph admits a proper TTG.*

Proof. Let G be the input graph. We use Lemmas 1–3 to construct the corresponding graph G' and path covering $P(G')$. Since G' contains G as its weak dual, if G' admits a straight-line drawing Γ, where all the faces are drawn as triangles, then Γ must be a proper TTG of G.

By construction G' has exactly three inner faces that are of length four (i.e., the quads). All the other faces are of length three. Consequently, if G' admits a straight-line drawing Γ, then all the inner faces except the three quads must be drawn as triangles. If the thee sticks of G' are stretched in Γ, then every face of Γ must be a triangle, and hence Γ must be a proper TTG of G. In other words, any planar embedding of G', where every path in $P(G')$ is stretched, must be a proper TTG of G.

It now suffices to prove that G' admits a planar embedding, where each path in $P(G')$ is stretchable. It is straightforward to verify that each subset of $P(G')$ with at least two paths has at least three free vertices. Hence by Theorem 1, G' admits a planar drawing, where every path in $P(G')$ is stretched; such a drawing can be computed by solving a barycentric system [5][2]. □

4 Proper TTG of Grid Graphs

In this section we give an algorithm to construct proper TTG for square grid graphs and parabolic grid graphs. Note that Gansner *et al.* [9] gave an algorithm to construct TTG for square grids and its subgraphs, where the outerface takes

[2] The authors believe that instead of relying on de Fraysseix and de Mendez's result [5], one can adapt well known straight-line planar graph drawing techniques (e.g. shift method [7]) to construct such a drawing of G' on an integer grid with small area.

the shape of an astroid, (also called cubocycloid), and hence the TTG was not proper. On the other hand, our algorithm constructs proper TTG for grid graphs and some of its subgraphs, as stated in the following theorem.

Theorem 3. *Let G be a planar graph with exactly four vertices of degree two. If G admits a rectangular grid drawing, then G also admits a proper TTG.*

Before proving Theorem 3, we show how to construct proper TTG of square grid graphs. A *square grid graph* $G_{m,n}$, where $m, n \geq 1$, is the graph determined by an integer grid I of dimension $m \times n$. By a vertex $u_{x,y}$ of $G_{m,n}$ we denote the vertex that correspond to the point (x, y) of I. See Fig. 5(a), where $u_{2,1}$ corresponds to the point c. We now introduce a few more definitions. By $x(v)$ (respectively, $y(v)$) we denote the x-coordinate (respectively, y-coordinate) of the point v. Let $v_1, v_2, \ldots, v_k$ be a polygonal chain such that $x(v_1) < x(v_2) < \ldots < x(v_k)$, $y(v_2) > y(v_3) > \ldots > y(v_k) > y(v_1)$ and $v_2, v_3, \ldots, v_k, v_2$ forms a strictly convex polygon; see Fig. 5(b). We call such a polygonal chain a *ripple of k vertices* and denote it by R_k.

Theorem 4. *Any square grid graph $G_{m,n}$, $m, n \geq 1$, admits a proper TTG.*

Proof. We first construct $G_{m,1}$ as follows. Construct a ripple $R_{m+2} = (v_1, v_2, \ldots, v_{m+2})$. Then add a point b below R_{m+2} and draw straight line segments from b to each vertex in R_{m+2}. We make sure that such that $x(b) = x(v_{m+2}) + \epsilon, \epsilon > 0$, and the drawing is planar. Now add a point t above R_{m+2} with $x(t) = x(v_2)$ and draw straight line segments from t to each vertex in R_{m+2}. We place t with sufficiently large y-coordinate so that the drawing remains planar and the vertices t, v_{m+2}, b become collinear. The resulting drawing is a proper TTG of $G_{m,1}$; see Fig. 5(c). Assume inductively that $G_{m,i}$, $i < n$, admits a proper TTG such that the following conditions hold.

(a) The topmost vertex t in the drawing is adjacent to a ripple R_{m+2} and the triangles incident to t correspond to the vertices of the ith row of $G_{m,i}$.
(b) The triangle below the edge $(v_j, v_{j+1}), 1 \leq j \leq m+1$, corresponds to the vertex $u_{j-1,i-1}$ of $G_{m,i}$.
(c) The bottommost vertex b of the drawing has the largest x coordinate in the drawing and it is adjacent to the leftmost and the rightmost vertices of R_{m+2}.
(d) One can decrease the y coordinate of b and redraw its adjacent edges to obtain another proper TTG of $G_{m,i}$.

Observe that the above conditions hold for the base case. We now construct the proper TTG of $G_{m,n}$ from the proper TTG Γ of $G_{m,n-1}$.

Let R_{m+2}=$(v_1, v_2, \ldots, v_{m+2})$ be the ripple that is adjacent to the topmost vertex t. Delete t from Γ to obtain another drawing Γ'. Now draw another ripple R'_{m+2}=$(v'_1(= v_1), v'_2, \ldots, v'_{m+2}(= v_{m+2}))$ such that $x(v'_2) = x(v_2)$, $y(v'_2) > y(v_2)$ and $v'_j, 2 < j < m+2$, is the midpoint of the line segment $v'_{j-1}v_j$; see Fig. 5(d). The triangles incident to R'_{m+2} correspond to a new row of m vertices, i.e, the $(n-1)$th row $G_{m,n}$. We now add a point t' above R'_{m+2} with $x(t')$=$x(v'_2)$ and draw straight line segments from t' to each vertex in R'_{m+2}. Conditions (c) and (d) help us to install t' with sufficiently large y-coordinate such that the drawing remains planar and the vertices t', v_{m+2} and the bottommost point b become collinear; see Fig. 5(e). It is straightforward to observe that the resulting drawing is the proper TTG of $G_{m,n}$ for which the conditions (a)–(d) hold. □

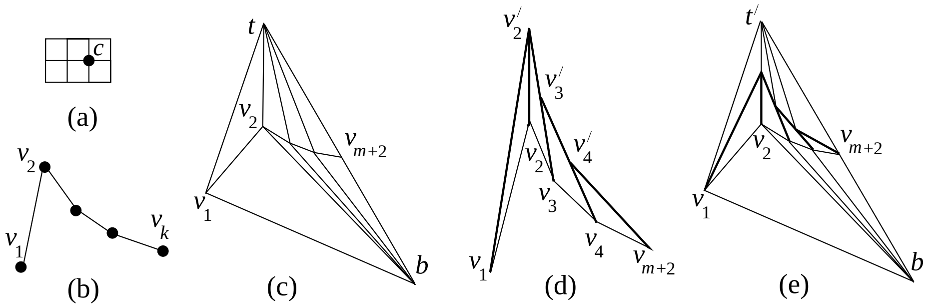

Fig. 5. (a) $G_{3,2}$. (b) R_5. (c) Proper TTG of $G_{m,1}$. (d) Construction of the triangles for the $(n-1)$th row of $G_{m,n}$. R'_{m+2} is shown in bold. (e) Installment of t'.

A *rectangular grid drawing* $\mathbb{G}_{m,n}$ is a planar drawing of some graph, where each vertex is drawn as a point on the $m \times n$ grid, each edge is drawn as either a horizontal or a vertical straight line segment and each face takes the shape of a rectangle. We now generalize the proof of Theorem 4 to prove Theorem 3.

*Proof (**Theorem 3**).* Let $\mathbb{G}_{m,n}$, $m, n>1$, be a rectangular grid drawing and let $\mathbb{G}_{m,j}$, $j \leq n$, be the subgraph of $\mathbb{G}_{m,n}$ induced by the vertices of the jth row and all the rows below it. A vertex u is *unsaturated* in $\mathbb{G}_{m,j}$ if u has a neighbor in $\mathbb{G}_{m,n}$ that does not belong to $\mathbb{G}_{m,j}$. Otherwise, u is *saturated* in $\mathbb{G}_{m,j}$.

We first construct a ripple R_k, where k is the number of vertices in the lowest row of $\mathbb{G}_{m,n}$. Observe that R_k is a TTG (not necessarily proper) of $\mathbb{G}_{m,0}$. We then incrementally construct the TTG $\Gamma_{m,i}$ (not necessarily proper) for $\mathbb{G}_{m,i}, i<n$, and finally add the triangles for the nth row such that the resulting drawing becomes a proper TTG of $\mathbb{G}_{m,n}$. While constructing $\Gamma_{m,i}$, $i<n$, we maintain the following invariants.

(a) Let $u_1, u_2, \ldots, u_t$ be the unsaturated vertices of $\mathbb{G}_{m,i}$. Then the outer boundary of $\Gamma_{m,i}$ while walking clockwise from the leftmost to the rightmost vertex of $\Gamma_{m,i}$ is a ripple $R_{t+1}=(v_1, v_2, \ldots, v_{t+1})$. The triangle below the edge $(v_j, v_{j+1}), 1 \leq j \leq t$, corresponds to the vertex u_j; see Figs. 9(d–f).

(b) The bottommost vertex b of the drawing has the largest x coordinate in the drawing and it is adjacent to the leftmost and the rightmost vertices of R_{t+1}.

(c) One can decrease the y coordinate of b and redraw its adjacent edges to obtain another TTG (not necessarily proper) of $G_{m,i}$.

Observe that the invariants are similar to invariants we used in the proof of Theorem 4. Consequently, we can install the nth row in a similar way, but we move the further detail of this construction in the Appendix. □

A *parabolic grid of n lines* is the graph determined by the arrangement of line segments $l_0, l_1, \ldots, l_n$, where l_i, $1 \leq i \leq n-1$, has endpoints at $(0, i)$ and

$(n-i, 0)$, and the endpoints of l_0 and l_n are $(0,0)$, $(n-1,0)$ and $(0, n-1)$, $(0,0)$, respectively. We can construct proper TTG for parabolic grid graphs in a way similar to the proof of Theorem 4; see the Appendix.

Theorem 5. *Every parabolic grid graph admits a proper TTG.*

5 Proper TTG for Plane Graphs with Max-Degree Four

Let G be a 3-connected plane graph with maximum degree four. We give an $O^*(4^{k_1}6^{k_2})$-time algorithm to decide whether G admits a proper TTG, where k_1 and k_2 are the number of inner vertices of degree four and the number of outer vertices in G, respectively.

Here is an outline of our algorithm. Given a 3-connected max-degree-4 plane graph G, we first construct a set of graphs $\mathcal{D}$ such that every graph $H \in \mathcal{D}$ contains G as its weak dual. We then prove that G admits a proper TTG if and only if some graph $H \in \mathcal{D}$ admits a straight-line drawing, where each face of H is a triangle; see Lemma 4. For each H we construct a set of feasible path coverings such that H admits a straight-line drawing with each face of H as a triangle if and only if one of these path coverings is stretchable; see Lemma 5. We show that the stretchability of each path covering can be tested in polynomial time; see Lemma 6. We show that $|\mathcal{D}| = O^*(2^{k_2})$ and the number of path coverings is $O^*(4^{k_1}3^{k_2})$. Therefore, the algorithm takes $O^*(4^{k_1}6^{k_2})$ time in total.

Let $w_1, w_2, \ldots, w_t$ be the outer vertices of G in clockwise order. Construct a graph G' by inserting G into a cycle $c_1, c_2, \ldots, c_t$ of t vertices and adding the edges (c_i, w_i), $1 \leq i \leq t$. Let G^* be the weak dual of G'; see Fig. 6(a). Consider now the set of graphs D that are obtained by contracting at most $t-3$ outer edges of G^*. Since G is 3-connected, D contains all the 3-connected plane graphs that contain G as their weak dual. For every graph $D' \in D$, we construct a set $D'_i, i \in \{0,1,2,3\}$, of $\binom{k_2}{i}$ graphs that are obtained from D' by subdividing i outer edges of D' (with one division vertex per edge); see Figs. 6(b–c). Let $\mathcal{D} = \bigcup_{\forall D' \in D}(D'_0 \cup D'_1 \cup D'_2 \cup D'_3)$. Observe that every graph that satisfies the following conditions belongs to $\mathcal{D}$.

(a) At most three outer vertices of H are of degree two.
(b) For every outer vertex v of degree two in H, if we contract an edge that is incident to v, then the resulting plane graph H' must be a 3-connected planar graph that contains G as its weak dual.

We now have the following lemma, whose proof is included in the Appendix.

Lemma 4. *The graph G admits a proper TTG if and only if some graph $H \in \mathcal{D}$ admits a straight-line drawing, where each face of H is a triangle.*

Let Γ be a straight line drawing of a plane graph H and let f be a face in Γ. By a *corner at v* in f we denote the angle at v interior to f, which is formed by the edges incident to v on f. A corner at v is *bold* if v is an internal vertex in Γ. A corner at v is *stretched* in Γ, if the corresponding angle is equal to 180°. A corner at v is *concave* in Γ, if the corresponding angle is greater than 180°.

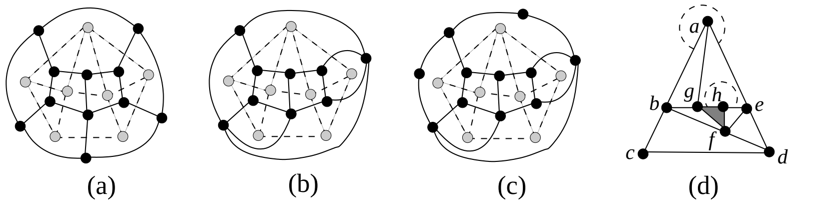

Fig. 6. (a) G and G^*, where G is shown in dashed lines. (b) A member D' of D. (c) A member of D'_2. (d) A straight-line drawing Γ, where a concave and a stretched corner is shown at vertex a and h, respectively. Every corner in Γ that is incident to an inner vertex (i.e., f, g or h) is a bold corner. All the inner faces in Γ are semi-outer except the shaded face, which is a full inner face.

We call an inner face f a *semi-outer face* of H, if f contains an outer vertex on its boundary. Otherwise, f is a *full-inner* face of H. See Fig. 6.

Observe that for every $H \in \mathcal{D}$, if f is a semi-outer face in H, then $\text{len}(f) \in \{3, 4, 5, 6\}$; Fig. 6(c) shows an example where each of these values appears at least once. For every other inner face f, $\text{len}(f) \in \{3, 4\}$. Moreover, if Γ is a straight-line drawing of H, where all the faces are drawn as triangles, then every face f in Γ contains exactly $\text{len}(f) - 3$ stretched corners. The following lemma computes an upper bound on the number of ways the corners of H can be stretched to have such a straight-line drawing. A detailed proof of this lemma is included in the Appendix.

Lemma 5. *The number of ways in which the corners of H can be stretched to obtain a straight-line drawing Γ such that every face f in Γ contains $len(f) - 3$ stretched corners is $O^*(4^{k_1}3^{k_2})$, where k_1 and k_2 are the number of inner vertices of degree four and the number of outer vertices in Γ, respectively.*

Every candidate of Lemma 5, marks some of the corners of H as "stretched". The following lemma shows how to test the feasibility of such a marking.

Lemma 6. *Let H be a graph that belongs to $\mathcal{D}$. Assume that for every face f in H, exactly $len(f) - 3$ corners of f are marked "stretched". Then one can decide in polynomial time whether H admits a straight-line drawing Γ, where all the corners marked "stretched" are stretched.*

Proof. If two different corners at the same vertex are marked stretched, then H cannot have a straight-line drawing such that both of those corners are stretched simultaneously. We thus assume that every vertex can have at most one corner that is marked stretched. We now construct a set P of paths, as follows.

- The three corners that are not marked on the outer face of H must be concave corners. Let the corresponding vertices be u, v and w in clockwise order on the outer face of H. Let S_{uv} be the path on the boundary of the outer face between the vertices u and v. Define S_{vw} and S_{wu} in a similar way. We add the paths S_{uv}, S_{vw} and S_{wu} to P.
- For every corner ϕ that is marked "stretched", we do the following. Let the vertex and edges that correspond to ϕ be v and $(v, x), (v, y)$, respectively. We add the path x, v, y to P.

- For every edge (x, y) of H, if (x, y) does not belong to any path of P, then we add the path x, y to P.
- For any two paths $u_1, u_2, \ldots, u_{k-1}, u_k$ and $v_1, v_2, \ldots, v_{t-1}, v_t$ in P, if $u_{k-1} = v_1$ and $u_k = v_2$, then we delete those paths from P and add the path $u_1, u_2, \ldots, u_{k-1}(= v_1), u_k(= v_2), \ldots, v_{t-1}, v_t$ to P. We assume that $u_1, u_2, \ldots, v_{t-1}, v_t$ do not create a cycle. Otherwise, each of the vertices on the cycle will contain a stretched corner and H will not have a straight-line drawing.

Observe that every edge in G is contained in a path of P. Furthermore, if H admits the required drawing Γ, then every path in P must be stretched in Γ. In the rest of the proof we show that every pair of paths in P is non-crossing and edge-disjoint, i.e., P is a path covering of H, and hence we can use Theorem 1 to test whether H admits the required straight-line drawing in polynomial time. The details for this part of the proof is included in the Appendix. $\square$

The following theorem is a consequence of Lemmas 4–6.

Theorem 6. *Let G be a 3-connected plane graph with maximum degree four. Then one can decide in $O^*(4^{k_1}6^{k_2})$-time whether G admits a proper TTG, where k_1 and k_2 are the number of inner vertices of degree four and the number of outer vertices in G, respectively.*

One can adapt the decision algorithm of this section for more general classes of plane graphs as follows. Let G be 3-connected plane graph of max-degree-Δ. Then one can construct a set of graphs $\mathcal{D}$ such that every graph $H \in \mathcal{D}$ contains G as its weak dual, and G admits a proper TTG if and only if some graph $H \in \mathcal{D}$ admits a straight-line drawing, where each face of H is a triangle. Observe that the cardinality of such a set is independent of Δ and $|\mathcal{D}| = O^*(2^{k_2})$. Since the proof of Lemma 6 does not depend on Δ, we can use the same lemma to construct necessary path coverings and to test the stretchability of those path coverings. Observe that the number of path coverings of H that we need to check is bounded by the number of ways we can mark the corners of H such that for every face f in H, exactly $\text{len}(f)-3$ corners of f are marked "stretched". Since $\text{len}(f) \leq \Delta + 2$, the number of path coverings is $O(\Delta^{3(k_1+k_2)})$, where k_1 is the number of inner vertices with degree greater than three. Consequently, the running time of the modified algorithm is $O^*(2^{k_2}\Delta^{3(k_1+k_2)})$, which is polynomial if $\Delta{=}O(1)$ and $k_1{+}k_2{=}O(\log n)$.

Theorem 7. *Let G be a 3-connected n-vertex plane graph with maximum degree Δ. Then one can decide in $O^*(2^{k_2}\Delta^{3(k_1+k_2)})$ time whether G admits a proper TTG, where k_1 and k_2 are the number of inner vertices of degree greater than three and the number of outer vertices in G, respectively.*

6 Conclusion and Open Problems

We presented algorithms for constructing proper TTG for 3-connected cubic planar graphs, and some grid graphs. Our results are strong in the sense that there exist 2-connected and 3-connected graphs with maximum degree four that do not admit proper TTG; see Fig. 1(g). We also described a fixed-parameter tractable decision algorithm for deciding proper TTG. In all these cases, one can obtain the proper TTG (if exists) by solving a barycentric system using the result of de Fraysseix and de Mendez [5]. Finding such representations on an integer grid with small area may be an interesting avenue to explore. The main open problem is of course whether deciding proper TTG is NP-hard, for general planar graphs, or whether there exists a polynomial-time algorithm.

Acknowledgments. We thank the organizers and participants in the 11th McGill-INRIA-Victoria Workshop on Computational Geometry 2012 for stimulating research discussions. We also thank many colleagues for discussions about this problem: Michael Kaufman, Martin Nöllenburg, Ignaz Rutter, Alexander Wolff, and many others.

References

1. M. J. Alam, J. Fowler, and S. G. Kobourov. Outerplanar graphs with proper touching triangle representation. Submitted to Graph Drawing 2012.
2. V. Batagelj. Inductive classes of cubic graphs. In *Proceedings of the 6th Hungarian Colloquium on Combinatorics, Eger, Hungary*, volume 37 of *Finite and infinite sets*, pages 89–101, 1981.
3. N. Bonichon, S. Felsner, and M. Mosbah. Convex drawings of 3-connected plane graphs. *Algorithmica*, 47(4):399–420, 2007.
4. A. Buchsbaum, E. Gansner, C. Procopiuc, and S. Venkatasubramanian. Rectangular layouts and contact graphs. *ACM Transactions on Algorithms*, 4(1), 2008.
5. H. de Fraysseix and P. O. de Mendez. Barycentric systems and stretchability. *Discrete Applied Mathematics*, 155(9):1079–1095, 2007.
6. H. de Fraysseix, P. O. de Mendez, and P. Rosenstiehl. On triangle contact graphs. *Combinatorics, Probability & Computing*, 3:233–246, 1994.
7. H. de Fraysseix, J. Pach, and R. Pollack. How to draw a planar graph on a grid. *Combinatorica*, 10:41–51, 1990.
8. C. Duncan, E. R. Gansner, Y. Hu, M. Kaufmann, and S. G. Kobourov. Optimal polygonal representation of planar graphs. *Algorithmica*, 63(3):672–691, 2012.
9. E. R. Gansner, Y. Hu, and S. G. Kobourov. On touching triangle graphs. In *Proceedings of the 18th International Symposium on Graph Drawing*, pages 250–261, 2010.
10. X. He. On finding the rectangular duals of planar triangular graphs. *SIAM Journal on Computing*, 22(6):1218–1226, 1993.
11. P. Koebe. Kontaktprobleme der konformen Abbildung. *Berichte über die Verhandlungen der Sächsischen Akademie der Wissenschaften zu Leipzig. Math.-Phys. Klasse*, 88:141–164, 1936.
12. C.-C. Liao, H.-I. Lu, and H.-C. Yen. Compact floor-planning via orderly spanning trees. *Journal of Algorithms*, 48:441–451, 2003.
13. R. Phillips. The Order-5 triangle partitions. `http://www.mathpuzzle.com/triangle.html`. [Online; accessed June 7, 2012].
14. M. Rahman, T. Nishizeki, and S. Ghosh. Rectangular drawings of planar graphs. *Journal of Algorithms*, 50(1):62–78, 2004.
15. C. Thomassen. Interval representations of planar graphs. *Journal of Combinatorial Theory (B)*, 40(1):9–20, 1986.

Appendix

Here we include detailed proofs of some claims with proof-sketches in the main body of the paper.

Proof of Lemma 3

Proof. Assume that the vertices w, v and u of $\mathcal{G}$ on which we apply Operation 3 corresponds to the faces T_1, T_2 and T_3 of $\mathcal{G}'$.

Case 1 (T_1, T_2 and T_3 are ordinary faces:) Without loss of generality assume that the outer boundary of the union of T_1, T_2 and T_3 is a, b, c, d, e; see Fig. 7(a). We add a vertex x interior to T_2 and then remove the edges (c, e) and (b, e). We now connect x with a, b, c, d, e. The resulting graph is G'; see Fig. 7(b). The new faces are ordinary and hence the quads and edges of G' coincide with that of $\mathcal{G}'$.

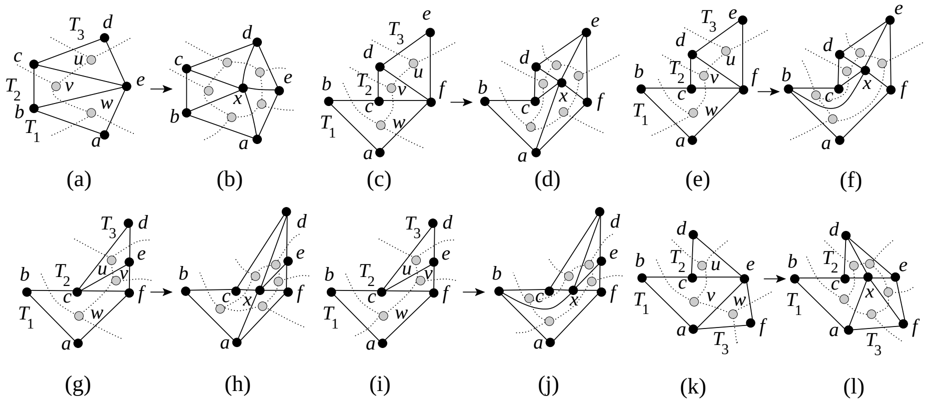

Fig. 7. (a–l) Illustration for Operation 3, $\mathcal{G}$ and G are shown in dotted lines as weak duals of $\mathcal{G}'$ and G', respectively.

Case 2 (Exactly one of T_1, T_2, T_3 is a quad): Without loss of generality assume that T_1 is the quad $[a, b, c, f]$ and $\langle b, c, f\rangle$ is its stick. By e' and e'' we denote the edges that are common to T_1, T_2 and T_2, T_3, respectively. We have two consider three subcases.

In Case 2.1 $e'' = (d, f)$. We add a vertex x interior to T_2 and then remove the edges (c, f) and (d, f). If (a, b) is the outer edge, then we connect x to a, c, d, e, f. If the outer edge is (a, f), then we connect x to b, c, d, e, f; see Fig. 7(c–f). The quad $[a, b, c, f]$ of $\mathcal{G}'$ does not determine quad for G'. The new quad of G' in Fig. 7(d) (respectively, Fig. 7(f)) is $[a, b, c, x]$ (respectively, $[a, b, x, f]$), where $\langle b, c, x\rangle$ (respectively, $\langle b, x, f\rangle$) is its stick.

In Case 2.2 $e'' = (c, e)$. We add a vertex x interior to T_2 and then remove the edges (c, e) and (c, f). If (a, b) is the outer edge, then we connect x to a, c, d, e, f.

If the outer edge is (a, f), then we connect x to b, c, d, e, f; see Fig. 7(g–j). The quad $[a, b, c, f]$ of $\mathcal{G}'$ does not determine quad for G'. The new quad of G' in Fig. 7(h) (respectively, Fig. 7(j)) is $[a, b, c, x]$ (respectively, $[a, b, x, f]$), where $\langle b, c, x\rangle$ (respectively, $\langle b, x, f\rangle$) is its stick.

In Case 2.3 e'' is empty, i.e., T_2, T_3 do not share any edge. We add a vertex x interior to T_2 and remove the edges (c, e) and (a, e). We then connect x to a, c, d, e, f; see Fig. 7(k–l). The quad $[a, b, c, e]$ of $\mathcal{G}'$ does not determine quad for G'. The new quad of G' in Fig. 7(l) is $[a, b, c, x]$, where $\langle b, c, x\rangle$ is its stick. Observe that in Fig. 7(k) T_2 is incident to edge (c, e). It is straightforward to obtain a similar analysis for the case when T_2 is incident to edge (b, c).

In Cases 2.1–2.3, the five new faces in G' correspond to the five vertices of the cycle that replace u, v and w in $\mathcal{G}$.

Case 3 (Exactly two of T_1, T_2, T_3 are quads): Without loss of generality assume that T_1 and T_2 are quads. We now have to consider four subcases depending on the variation in the edge sharing of these faces.

In Case 3.1 T_1 and T_3 share the edge (a, f); see Fig. 8(a). The outer edges of $\mathcal{G}'$ are (a, b) and (b, c). The paths $\langle b, e, f\rangle$ and $\langle c, d, e\rangle$ are the sticks of T_1 and T_2, respectively. We add a vertex x interior to T_2, remove the edges $(b, e), (a, f)$ and then connect x to b, d, e, f, g; see Fig. 8(b). The quads $[b, c, d, e]$ and $[a, b, e, f]$ of $\mathcal{G}'$ do not determine quads for G'. The new quads of G' are $[b, c, d, x]$ and $[a, b, x, g]$, where $\langle c, d, x\rangle$ and $\langle b, x, g\rangle$ are their sticks, respectively. Observe that the five new faces in G' correspond to the five vertices of the cycle that replace u, v and w in $\mathcal{G}$. By the inductive hypothesis, no two sticks of $\mathcal{G}'$ have an edge in common. Therefore, edge (c, d) cannot be a part of any other sticks in $\mathcal{G}'$. Consequently, no two sticks of G' can have an edge in common.

In Case 3.2 T_2 and T_3 share the edge (c, e); see Fig. 8(c). The outer edges are (a, b) and (b, c). The paths $\langle b, f, g\rangle$ and $\langle e, c, f\rangle$ are the sticks of T_1 and T_2, respectively. We now add a vertex x interior to T_2, remove the edges $(b, f), (c, e)$ and then connect x to b, d, e, f, g; see Fig. 8(d). The quads $[b, c, e, f]$ and $[a, b, f, g]$ of $\mathcal{G}'$ do not determine quads for G'. The new quads of G' are $[b, c, d, x]$ and $[a, b, x, g]$. By the inductive hypothesis, $\mathcal{G}'$ has exactly three sticks. Both (c, d) and (a, g) cannot be contained in the third stick of $\mathcal{G}'$ since this will imply that $[c, d = g, a]$ is a quad of $\mathcal{G}'$. But $[c, d = g, a]$ cannot be a quad since by definition every quad must be a 4-cycle. If (c, d) is a part of the third stick, we then define $\langle x, g, a\rangle$ and $\langle d, x, b\rangle$ as the sticks of T_1 and T_2, respectively. Otherwise, we define $\langle b, x, g\rangle$ and $\langle c, d, x\rangle$ as the sticks of T_1 and T_2, respectively.

In Case 3.3 T_2 and T_3 share the edge (d, f); see Fig. 8(e). The outer edges are (a, b) and (b, c). The paths $\langle b, f, g\rangle$ and $\langle c, d, f\rangle$ are the sticks of T_1 and T_2, respectively. We now add a vertex x interior to T_2, remove the edges $(b, f), (d, f)$ and then connect x to b, d, e, f, g; see Fig. 8(f). The quads $[a, b, f, g]$ and $[b, c, d, f]$ of $\mathcal{G}'$ do not determine quads for G'. The new quads of G' are $[a, b, x, g]$ and $[b, c, d, x]$, where $\langle b, x, g\rangle$ and $\langle c, d, x\rangle$ are their sticks, respectively. Observe that the five new faces in G' correspond to the five vertices of the cycle that replace u, v and w in $\mathcal{G}$. By the inductive hypothesis, no two sticks of $\mathcal{G}'$ have an edge

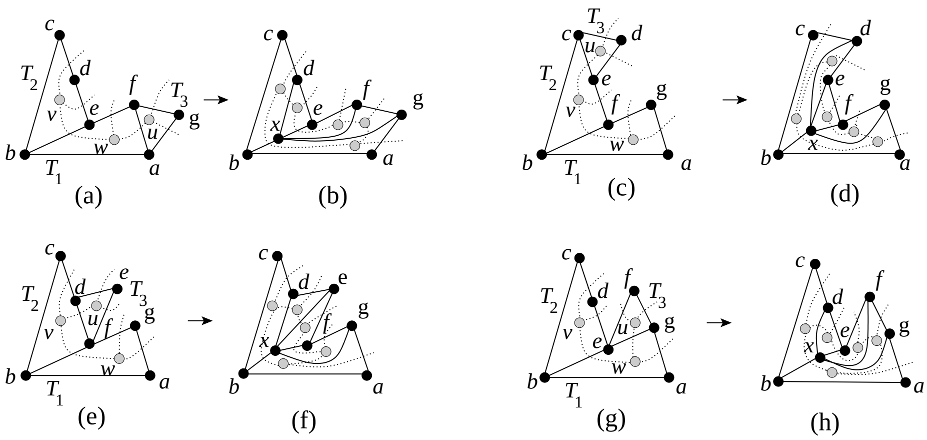

Fig. 8. (a)–(h) Illustration for Case 3, when T_1 and T_2 are quads.

in common. Therefore, edge (c, d) cannot be a part of any other sticks in $\mathcal{G}'$. Consequently, no two sticks of G' can have an edge in common.

In Case 3.4 T_1 and T_3 share the edge (e, g); see Fig. 8(g). The outer edges are (a, b) and (b, c). The paths $\langle b, e, g\rangle$ and $\langle c, d, e\rangle$ are the sticks of T_1 and T_2, respectively. We now add a vertex x interior to T_2, remove the edges $(b, e), (e, g)$ and then connect x to b, d, e, f, g; see Fig. 8(f). The quads $[a, b, e, g]$ and $[b, c, d, e]$ of $\mathcal{G}'$ do not determine quads for G'. The new quads of G' are $[a, b, x, g]$ and $[b, c, d, x]$, where $\langle b, x, g\rangle$ and $\langle c, d, x\rangle$ are their sticks, respectively. Observe that the five new faces in G' correspond to the five vertices of the cycle that replace u, v and w in $\mathcal{G}$. By the inductive hypothesis, no two sticks of $\mathcal{G}'$ have an edge in common. Therefore, edge (c, d) cannot be a part of any other sticks in $\mathcal{G}'$. Consequently, no two sticks of G' can have an edge in common.

Note that one last potential case (when all the T_1, T_2 and T_3 are quads) does not arise since in this case we cannot apply Operation 3 on the corresponding vertices w, v, u in $\mathcal{G}$. □

Proof of Theorem 3

Proof. This is the continuation of the proof of Theorem 3 presented in the main body of the paper.

Assume inductively that we have constructed $\Gamma_{m,i}$, where $i < n-1$. We now describe how to install the triangles for the vertex set $Z = \{z_1, z_2, \ldots, z_p\}$ of the $(i+1)$th row maintaining (a)–(d). Let $u'_1, u'_2, \ldots, u'_{t'}$ be the unsaturated vertices of $\mathbb{G}_{m,i+1}$. We create a ripple $R'_{t'+1}{=}(v'_1(= v_1), v'_2, \ldots, v'_{t'+1}(= v_{t+1}))$ as follows.

If z_1 has the smallest x-coordinate in $\mathbb{G}_{m,n}$, then we add a point v'_2 above R_{t+1} with $x(v_1){<}x(v'_2){<}x(v_2)$, and draw the straight line v'_2v_2 avoiding any edge crossing; see Fig. 9(b). We now iterate the following steps starting with $j = 3$ and $k = 3$, as long as $j \leq p$.

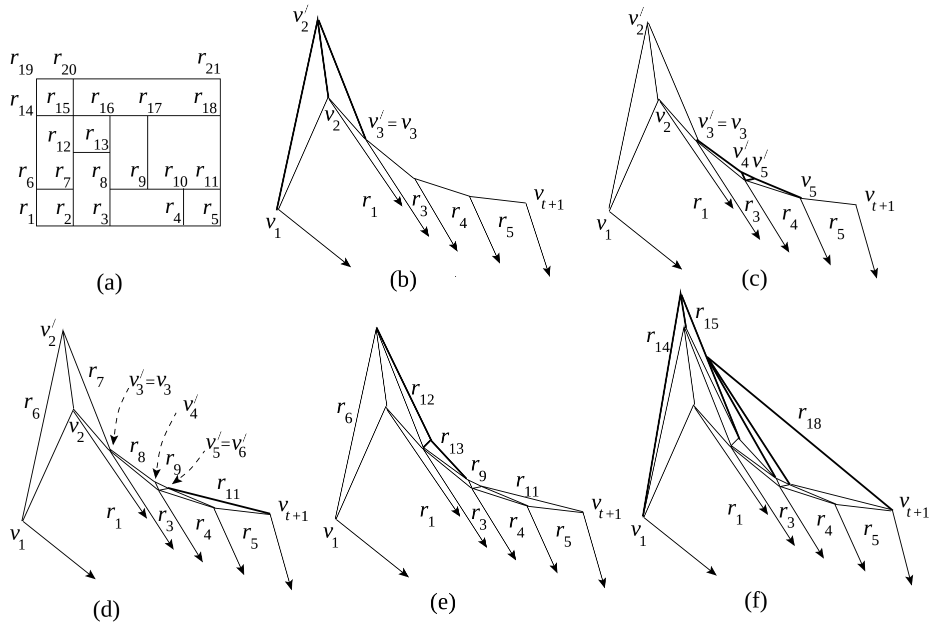

Fig. 9. (a) A rectangular grid drawing $\mathbb{G}_{5,4}$. (b–d) Installation of the 1st row $Z = r_6, r_7, \ldots, r_{11}$ on top of the TTG for $\mathbb{G}_{m,0}$. The triangles for $r_8, \ldots, r_{10}$ and r_{11} are constructed by Steps (ii) and (iii), respectively. (e) Installation of the 2nd row $Z = r_{12}, r_{13}$. (f) Installation of the 3rd row $Z = r_{14}, \ldots, r_{18}$. The triangles for r_{16}, r_{17}, r_{18} are constructed by Step (iv).

(i) If z_j does not have any downward neighbor, then we increment j by 1 for the next iteration.

(ii) If z_{j-1}, z_j are not adjacent, then z_j must be unsaturated. Here the point v'_j coincides with v_k, and we increment k by 1; see v'_3 in Fig. 9(b). Let z_q be the first vertex after z_j that has a downward neighbor. Assume that $w = q - j$ and set $j = q$. We place the points $v'_j, v'_{j-1}, v'_{j-2}, \ldots, v_{j'-w+1}$ such that they become a part of the ripple, and draw the straight lines from v_k to the newly added points; see v'_4, v'_5 in Fig. 9(c). If z_j and z_{j+1} are adjacent, then we increment k by 2; otherwise, we increment k by 1. Finally, we increment j by 1 for the next iteration.

(iii) If z_{j-1}, z_j are adjacent and z_j is unsaturated, then

- If both z_{j-1} and z_j have downward neighbors, then we examine whether z_{j-1} is saturated. If z_{j-1} is saturated, then the point v'_j coincides with v'_{j-1}. We draw the line segment $v'_j v_k$ and increment k and j by 1 for the next iteration; see the triangle for r_{11} in Fig. 9(d). If z_{j-1} is unsaturated, then we place the point v'_j in the middle of the line segment between the last point placed and the point v_k; see the triangles for r_{15} and r_{16} in Fig. 9(f). We then increment k and j by 1 for the next iteration.

- If z_j does not have downward neighbor, then let z_q be the first vertex after z_j that has a downward neighbor. Assume that $w = q - j$ and set $j = q$. We place the points $v'_j, v'_{j-1}, v'_{j-2}, \ldots, v_{j'-w+1}$ such that they become a part of the ripple, and draw the straight lines from v_{k-1} to the newly added points; which is similar to Fig. 9(c). We then increment k and j by 1 for the next iteration.

(iv) If z_j is saturated, then we examine whether z_{j-1} is saturated. If z_{j-1} is saturated, then the point v'_j coincides with the last point placed, and we add the straight line $v'_j v_k$, and increment k and j by 1 for the next iteration; see the triangles for r_{16}, r_{17} and r_{18} in Fig. 9(f). Otherwise, z_{j-1} is unsaturated and we place the point v'_j in the middle of the line segment between the last point placed and the point v_k; see the triangles for r_{15} and r_{16} in Fig. 9(f). We then increment k and j by 1 for the next iteration.

The case analysis when z_1 does not have the smallest x-coordinate in $\mathbb{G}_{m,n}$ is similar. The only difference is the first few vertices of $R'_{t'+1}$ coincides with that of R_{t+1}, as shown in Fig. 9(e).

To create the triangles for the nth row, we add a point t above the TTG of $\mathbb{G}_{m,n-1}$ with $x(t)=x(v_2)$, where v_2 is the second vertex of the ripple on the outer face of $\mathbb{G}_{m,n-1}$, and draw straight line segments from t to each vertex of the ripple. Conditions (b) and (c) of the induction invariant help us to install t with sufficiently large y-coordinate such that the drawing remains planar and the vertices t, v_{m+2} and the bottommost point b of the drawing become collinear. □

Parabolic Grid

We define parabolic grid graphs as follows. Let $L = \{l_0, l_1, l_2, \ldots, l_n\}$ be a set of $n + 1$ line segments where line segment l_i, $1 \leq i \leq n - 1$, has endpoints at $(0, i)$ and $(n - i, 0)$. The endpoints of l_0 are $(0, 0)$, $(n - 1, 0)$ and the endpoints of l_n are $(0, n - 1), (0, 0)$. We denote the coordinate of the intersection point of lines l_i and l_j as (i, j). We place a vertex to each intersection point. The vertex on the point (i, j) is denoted by $v_{i,j}$. The resulting graph is the *parabolic grid graph* of size n which we denote by G_n; see Fig. 10.

To prove Theorem 5, we define the following term. Let $R_k = v_1, v_2, \ldots, v_k$ be a ripple. Let the middle point of the line segment $v_1 v_2$ be v'. We then call the polygonal chain $v_1, v', v_2, \ldots, v_k$ an *extended ripple* and denote by $\mathbb{R}_{k+1}$. We are now ready to prove Theorem 5.

Proof of Theorem 5

Proof. We first construct proper TTG of G_2 by placing a point d inside a triangle abc and connecting d to each of a, b, c. Without loss of generality we assume that $x(a) < x(c) < x(b)$ and $y(c) > y(a) > y(b)$. We now construct a proper TTG for G_3 from the proper TTG of G_2. We remove the vertex c and its incident edges. We then add extended ripple $\mathbb{R}_4 = v_1, v_2, v_3, v_4$ such that v_1 and v_4 coincides with a and b, respectively. We now connect v_3, d. We then place the vertex c

above $\mathbb{R}_3$ and connect c to all the vertices of $\mathbb{R}_3$. Assume inductively that G_i, $3 \leq i < n$, admits a proper TTG such that the following conditions hold.

(a) The topmost vertex c in the drawing is adjacent to an extended ripple $\mathbb{R}_{i+1}$ and the triangles incident to c correspond to the vertices on l_i of G_i.
(b) The triangle below the edge $(v_j, v_{j+1}), 3 \leq j \leq i-1$, corresponds to the vertex $u_{i-1,i-j}$ of G_i and the triangle below the edges (v_1, v_2) and (v_2, v_3) corresponds to the vertex $u_{i-1,i-2}$ of G_i.
(c) The bottommost vertex b of the drawing has the largest x coordinate in the drawing and a has the smallest x coordinate.

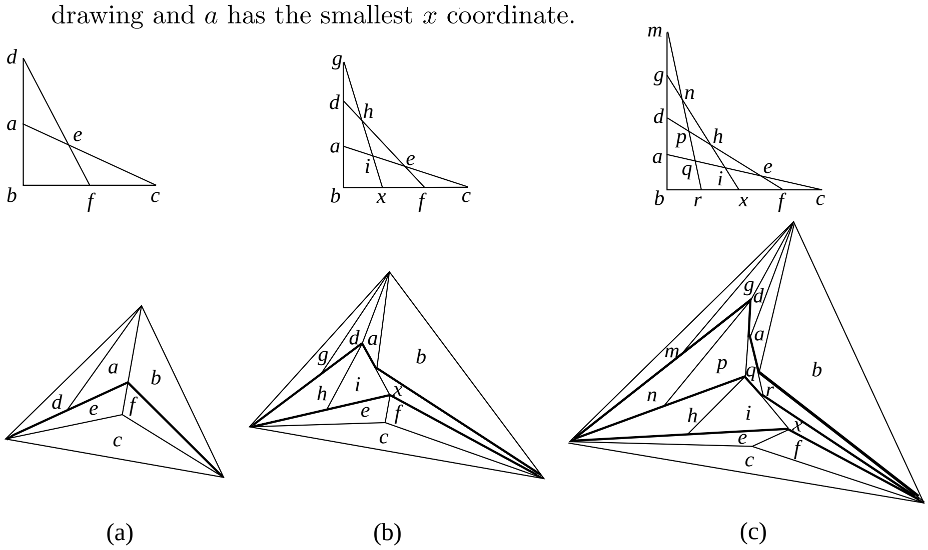

Fig. 10. (a–c) Construction of proper TTG for parabolic grid graphs. Extended ripples are shown in bold. (a) G_3 and its proper TTG, (b) G_4 and its proper TTG, and (c) G_5 and its proper TTG.

We now construct a proper TTG of G_n from proper TTG of G_{n-1} such that the invariants (a)–(c) hold. Let the extended ripple $\mathbb{R}_n$ that is adjacent to the vertex c in the TTG of G_{n-1} be $v'_1, v'_2, \ldots, v'_n$. We remove the vertex c and its incident edges. We then add extended ripple $\mathbb{R}_{n+1} = v_1, v_2, \ldots, v_{n+1}$ such that v_1 and v_{n+1} coincides with a and b, respectively and v_{j+1}, $3 \leq j \leq n-2$, is the middle point of the line segment $v'_j v_j$. We now add the edges (v'_j, v_j) for $3 \leq j \leq n-1$. We then place the vertex c above $\mathbb{R}_{n+1}$ and connect c to all the vertices of $\mathbb{R}_{n+1}$. It is easy to check that the invariants hold for the constructed proper TTG of G_n. See Fig. 10 for an illustration of the proof. □

Proof of Lemma 4

Proof. If some graph $H \in \mathcal{D}$ admits a straight-line drawing such that each face of H is a triangle, then the drawing itself is a proper TTG of G. Hence, we assume that G admits a proper TTG Γ and then prove that the graph G_Γ corresponding to Γ belongs to $\mathcal{D}$. Observe that G is the weak dual of G_Γ. If G_Γ is 3-connected, then $G_\Gamma \in D \subset \mathcal{D}$ by construction. Otherwise, G_Γ is not three connected and we now prove that G_Γ satisfies (a) and (b).

If G_Γ does not satisfy (a), then G_Γ contains four or more outer vertices of degree two. These vertices correspond to four or more corners in Γ, contradicting that Γ is a proper TTG. Therefore, it remains to prove that G_Γ satisfies (b). Let G'_Γ be the graph obtained by contracting an incident edge for each outer vertex of degree two in G_Γ. Since G_Γ contains G as its weak dual and the contraction operations do not change the corresponding faces, G must be a weak dual of G'_Γ. Since G'_Γ contains a 3-connected graph as its weak dual and does not contain any outer vertex of degree two, G'_Γ must be a 3-connected graph. □

Proof of Lemma 5

Proof. Let f be a face of H. If f is an outer face with $i \in \{0, 1, 2, 3\}$ vertices of degree two, then we can choose the three concave corners of Γ in $\binom{k}{3-i}$ ways, where k is the number of outer vertices in H. All the corners interior to f other than the concave corners must be stretched.

Assume that f is an inner face of H. If $\text{len}(f) = 3$, then f cannot have any stretched corner. Otherwise, $\text{len}(f) = 4$. If f is a full-inner face, then exactly one of its four bold corners must be stretched. Otherwise, f is a semi-outer face. In this case f cannot have a vertex of degree two since this will imply the vertex in G corresponding to f is a vertex of degree two; see Fig. 11(a). We may thus assume that f contains $i \in \{1, 2\}$, outer vertices. Then exactly one of its $4 - i$ bold corners must be stretched; see Fig. 11(b).

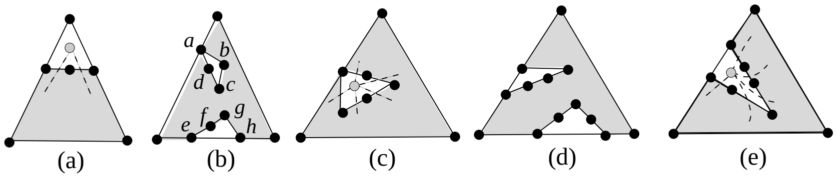

Fig. 11. (a–b) Illustration for the case when $\text{len}(f) = 4$. The corners at b, c, d, g and f are bold corners. Illustration for the case when (c–d) $\text{len}(f) = 5$ and (e) $\text{len}(f) = 6$.

Assume now that $\text{len}(f) \geq 5$. Since the maximum degree of G is four, f must be a semi-outer face. If f contains a vertex of degree two, then all the bold corners must be stretched. Otherwise, f contains $i \in \{1, 2\}$, outer vertices. Observe that i cannot be one since this will imply the vertex in G corresponding to f is a vertex of degree five or more; see Fig. 11(c). Therefore, if $\text{len}(f) = 5$ and $i = 2$, then two of the three bold corners of f must be stretched; see Fig. 11(d). Otherwise, $\text{len}(f) = 6$ and $i = 2$. This case will imply the vertex in G corresponding to f is a vertex of degree five; see Fig. 11(e).

Observe that for each semi-outer (respectively, full-inner) face, the maximum number of ways to mark the corners as "stretched" is at most three (respectively, four). Since the semi-outer faces correspond to the outer vertices of G and the full-inner faces correspond to the internal vertices of G, the number of ways in which the corners can be stretched in Γ is $O^*(4^{k_1} 3^{k_2})$, where k_1 and k_2 are the number of inner vertices of degree four and the number of outer vertices in H, respectively. □

Proof of Lemma 6

Proof. This is the continuation of the proof of Lemma 6 presented in the main body of the paper.

Observe that every edge in G is contained in a path of P. Furthermore, if H admits the required drawing Γ, then every path in P must be stretched in Γ. In the following we show that every pair of paths in P is non-crossing and edge-disjoint, i.e., P is a path covering of H, and hence we can use Theorem 1 to test whether H admits the required straight-line drawing in polynomial time.

Let p_1 and p_2 be two paths in P. We now prove that p_1 and p_2 are non-crossing and edge-disjoint. Suppose for a contradiction that p_1 and p_2 cross. If they have an internal vertex v in common, then v must have two different corners that are marked stretched, which contradicts our initial assumption that every vertex can have at most one corner that is marked stretched; see in Figs. 12(a–c). We may thus assume that p_1 and p_2 have an edge (u, v) in common, where none of u and v is internal to both p_1 and p_2. We now have the following cases.

Case 1: Both of the vertices u and v are end vertices of p_1. In this case p_1 is an edge that is contained in p_2. By construction, such a case cannot appear.

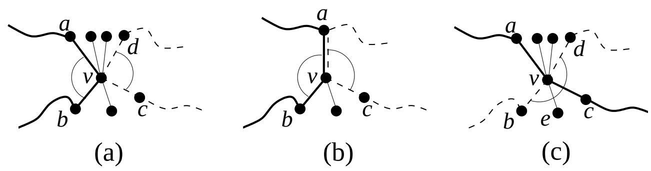

Fig. 12. (a–b) The paths p_1 and p_2 have an internal vertex in common, where p_1 and p_2 are shown in bold and dashed lines, respectively. The corners that are marked stretched are denoted by circular arcs. (c) The paths p_1 and p_2 cannot cross in this way, since no corner (therefore, corner $\angle bvd$) can have an edge that splits the corner.

Case 2: One of the vertices u and v is an internal vertex in p_1. Without loss of generality assume that u is an internal vertex of p_1. If v is also an internal vertex of p_1, then u and v must be the end vertices of p_2 and we can use Case 1 to obtain a contradiction. Therefore, we assume that v is an end vertex of p_1. Since u is an internal vertex in p_1, u must be an end vertex of p_2. The vertex v cannot be an end vertex of p_2 since in that case both u and v must be the end vertices of p_2 deriving a contradiction. Therefore, we assume that v is an internal vertex of p_2. Observe that p_1 and p_2 have the following form: $p_1 = (u_1, u_2, \ldots, u_{k-1}(= u), u_k(= v))$ and $p_1 = (v_1(= u), v_2(= v), \ldots, v_{t-1}, v_t)$. By the construction of P, such a case cannot appear.

Since any two paths in P are non-crossing and edge-disjoint, P is a path covering of H. Therefore, we can use Theorem 1 to test whether H admits the required straight-line drawing Γ in polynomial time. □